IOP Conf. Series: Materials Science and Engineering **107** (2016) 012033 doi:10.1088/1757-899X/107/1/012033

Synthesis of $LiNi_xMn_{2-x}O_4$ by low-temperature solid-state reaction and its microstructure

D Purwaningsih[1,2*], R Roto[1] and H Sutrisno[2]

[1]Department of Chemistry, Faculty of Mathematics and Natural Sciences, Gadjah Mada University, Sekip Utara BLS 21, Yogyakarta 55584 Indonesia
[2]Department of Chemistry Education, Faculty of Mathematics and Natural Sciences, Yogyakarta State University, Jl. Colombo 1, Yogyakarta 55281 Indonesia

[*]E-mail: dyahuny@yahoo.com

Abstract. This study aims to synthesis the Ni-doped $LiNi_xMn_{2-x}O_4$ (x = 0; 0.02; 0.04; 0.06; 0.08; 0.1) by low temperature solid-state reaction. The microstructure of the product was evaluated based on the mole ratio of Ni/Mn of the precursors. The structural analysis of $LiNi_xMn_{2-x}O_4$ was analyzed by x-ray diffraction equipped with the Direct Method of win PLOTR package program and Diamond. It was found that doping with Ni could change the size, crystallinity and microstructure of $LiNi_xMn_{2-x}O_4$. The $LiNi_xMn_{2-x}O_4$ solids have a cubic structure with a space group of *Fd3m*. The increase in the doping content does not affect the structure. The particle size of the products is about 150-500 nm. The crystallinity of the solids tends to increase with the increase in Ni content. However, the increase of Ni content in the product causes the lattice parameters of the unit cell to decrease.

1. Introduction

Lithium-ion batteries are widely used for energy storage, portable devices, and electric vehicles. Although many new cathode materials are developed, $LiMn_2O_4$ is still well recognized as a promising cathode material for these batteries [1]. The spinel-structured $LiMn_2O_4$ offers attractive alternative material over commercially available $LiCoO_2$. $LiMn_2O_4$ is cheap, non-toxic, and safe [2]. However, it has severe capacity fading in the application [3]. The charge-discharge cycling capability of $LiMn_2O_4$ at high temperatures can be improved by the substitution of Mn by other transition metals to give the corresponding $LiM_xMn_{2-x}O_4$ where M = Co, Mg, Al, Cr, Ni, Fe, Ti and Zn [4]. $LiNi_xMn_{2-x}O_4$has a discharge capacity of 140 $mAhg^{-1}$ and open circuit potential of 4.7 V. This energy density is tunable by doping [5].

It is documented well that electrochemical performance of the battery cathode is affected by the powder properties such as structure, particle size, grain morphology, specific surface area and crystallinity [6]. In addition to its large surface area, fast transport of mass and charge, there are many properties to explore. The large surface area and small particle size can improve solubility in the electrolyte. The alteration in chemical properties may make the electrode materials sensitive to the presence of impurities[7].

The electrochemical property of $LiMn_2O_4$–based spinel highly depends on its synthetic routes, such as the Pechini process, sol-gel, emulsion method, the citric method [8], etc. However, most of these

methods involve many treatment processes or expensive reagent, which is time-consuming and high cost for commercial applications. We report here on the synthesis of series of $LiNi_xMn_{2-x}O_4$ using a low-temperature solid-state reaction at various Ni/Mn mole ratios. The physical properties and microstructures of the synthesized materials were investigated.

2. Experimental Section

2.1. Synthesis of MnO_2 and $LiNi_xMn_{2-x}O_4$.

An analytical grade of $Mn(CH_3COO)_2$ and $Na_2S_2O_8$ (Aldrich) were used. All other chemicals were used without further purification. In a typical synthesis, $Mn(CH_3COO)_2$ and $Na_2S_2O_8$ with a molar ratio of 1:1 were dissolved at room temperature in 80 mL deionized distilled water. The mixture was stirred to form a clear homogeneous solution. The solution was transferred to the flask and heated at 120 ^oC for 12 h. The obtained powder was subsequently dried at 300 ^oC for 1 h in the oven.

Synthesis of $LiNi_xMn_{2-x}O_4$. is the following; LiOH of 0.00143 moles, 0.0000286 moles of $Ni(CH_3COO)_2$ and 0.0028314 moles were dispersed into high purity ethanol to form a thick slurry and stirred. The product was separated and dried at room temperature. The above process was repeated three times. The $LiNi_{0.02}Mn_{1.98}O_4$ powder was ignited at 750 ^oC for 10 hours. The same procedure was followed for synthesizing the materials with different mole ratio.

2.2. Characterization of the $LiNi_xMn_{2-x}O_4$ microstructure.

The obtained MnO_2 and $LiNi_xMn_{2-x}O_4$powders were analyzed using X-ray powder diffractometer (XRD). The XRD patterns were obtained on Rigaku Miniflex 600-Benchtop XRD instrument using Cu Kα radiation (λ = 1.5406 Å) at ambient temperature. The XRD instrument was set to operate at 40 kV and 15 mA. The XRD data was obtained with a 2Θ interval ranging from 20^o to 90^o. The Rietveld analysis was conducted with the Fullprof software package [9] to refine the X-ray diffraction data. The refined parameters are a unit cell, scale factor and full width at half-maximum (FWHM). The SEM images were obtained using JEOL JSM-6510LASEM. The effect of the nickel content on the structure of $LiMn_2O_4$ was studied using energy dispersive X-ray spectroscopy (EDX). The EDX analysis was also used to analyze the presence of Mn, O and Ni elements in the prepared materials. The Brunauer-Emmett-Teller (BET) data was collected based on adsorption data in relative pressure (P/Po) of about 0.30 [10]. The BET calculation was done in ASAP 2020 V4.01 software from Micrometrics.

3. Results and discussion

3.1. XRD Patterns

Figure1 shows XRD patterns of produced $LiNi_xMn_{2-x}O_4$. High peak intensity suggests that the $LiNi_xMn_{2-x}O_4$ has good crystallinity. Figure 2 shows the variation of the lattice constant of the materials with different compositions. The Rietveld refinement data obtained using Full Prof indicates that lattice parameter decreases with the increase in doping content. The substitution of Mn^{3+} by Ni^{2+} in the octahedral sites leads to the decrease in the lattice parameters. Note that ionic radius of Ni^{2+} is 0.560 Å, smaller than that of Mn^{3+}, which is 0.645 Å. The difference in the ionic radius between Ni^{2+} and Mn^{3+} is small, therefore only a few of change the lattice parameter.

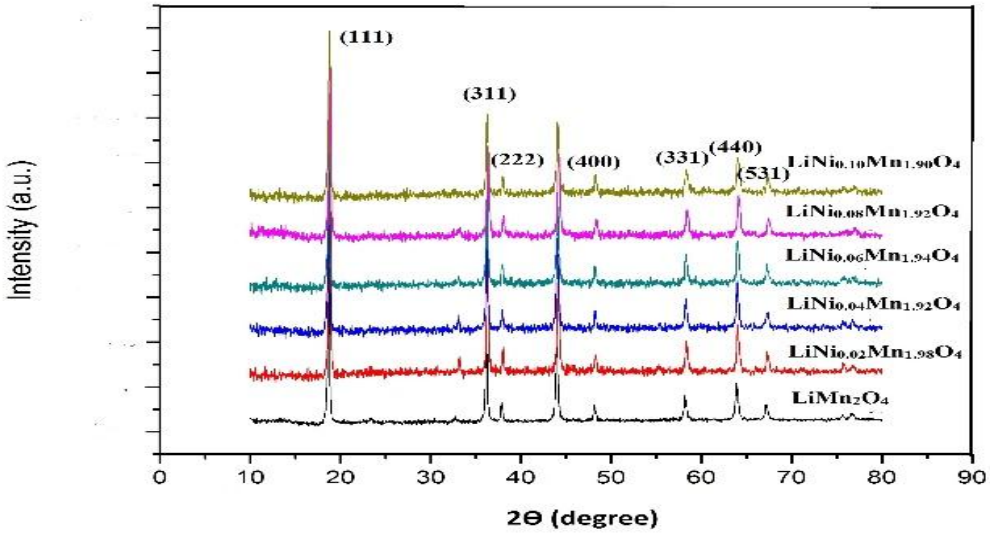

Figure 1. XRD Patterns of $LiNi_xMn_{2-x}O_4$ Ni/Mn mole ratios

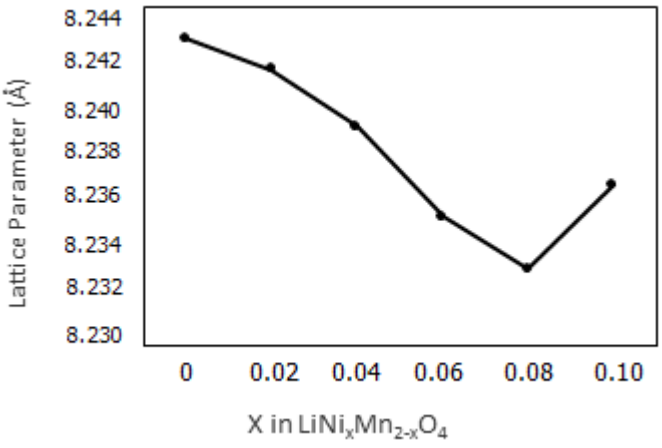

Figure 2. Variation of lattice parameter with x in $LiNi_xMn_{2-x}O_4$

Figure 3 shows the XRD patterns of $LiNi_xMn_{2-x}O_4$. The products have a cubic phase with space group of *Fd3m* as indicated by results of analysis using winPLOTR package program and Diamond. The results of Rietveld are shown in Fig. 3. The experimental points are given as dot (.) and theoretical data are shown as solid line. The difference between theoretical and experimental data is shown as a bottom line. The vertical lines represent the Bragg's allowed peaks. The X-ray diffraction data show at 31-33^o, which can be assigned to a Mn_2O_3 phase. The presence of Ni in the structure causes the appearance of $NiMnO_3$, which is indicated by the presence of the peaks at 31-33^o [11]. It seems that lithium ions occupy the tetrahedral (8a) site. After the modification, the lattice shrinkage is due to the smaller ionic radii of $Ni^{2+,}$ which replaced the Mn^{3+} at 16d sites. On the other hand, Ni^{2+} substituting part Mn^{3+} can enhance the content of Mn^{4+} to keep the charge balance, and Mn^{4+} is with smaller ionic radii than that of Mn^{3+} [12]. Oxygen atoms are arranged in the cubic-closed packing 32e.

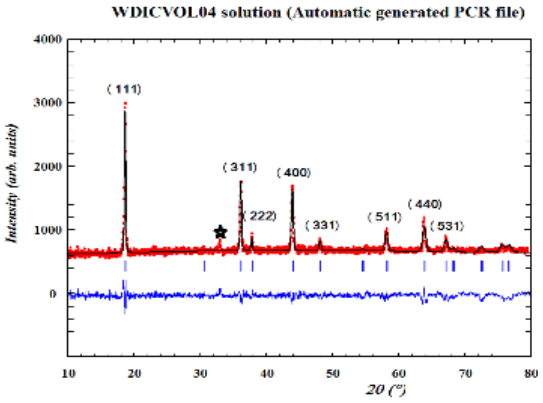

$LiMn_2O_4$

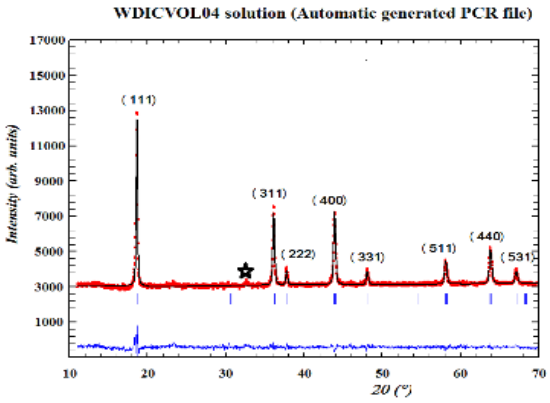

$LiNi_{0.02}Mn_{1.98}O_4$

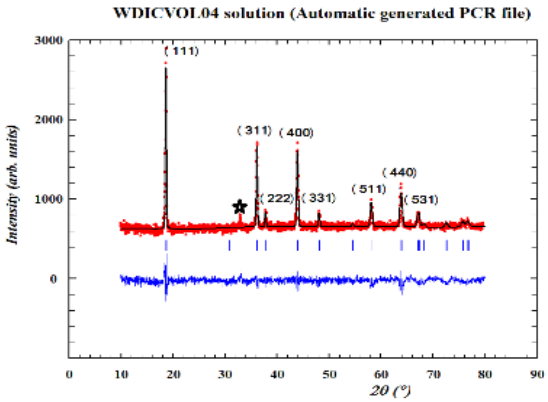

$LiNi_{0.04}Mn_{1.96}O_4$

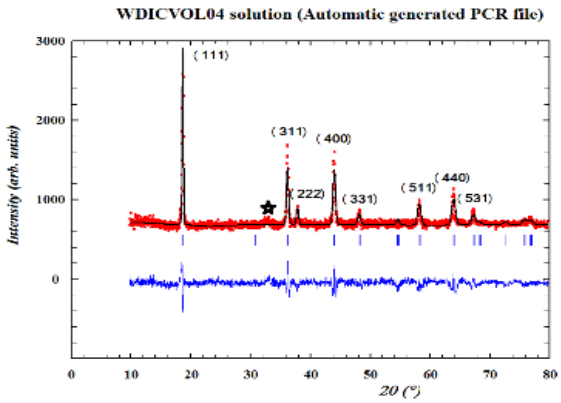

$LiNi_{0.06}Mn_{1.94}O_4$

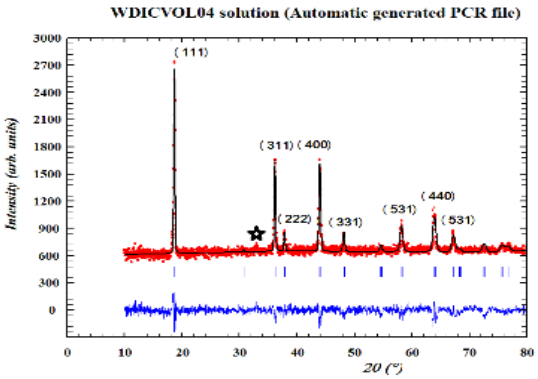

$LiNi_{0.08}Mn_{1.92}O_4$

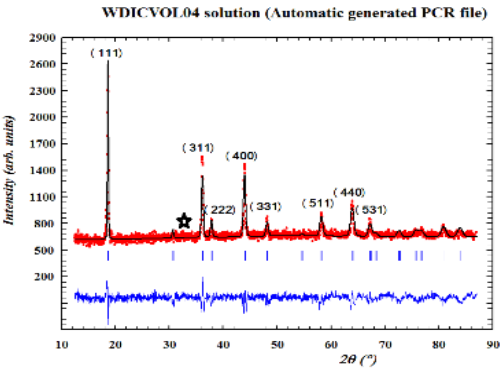

$LiNi_{0.10}Mn_{1.90}O_4$

Figure 3 XRD refinement data of $LiNi_xMn_{2-x}O_4$ with various Ni/Mn mole ratios

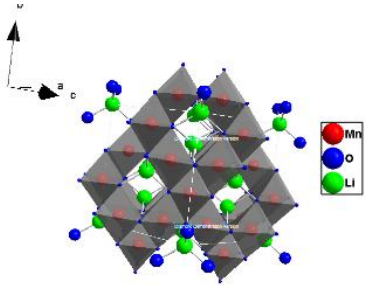

Figure 4. Microstructure of $LiNi_{0.1}Mn_{1.9}O_4$

3.2. SEM Images

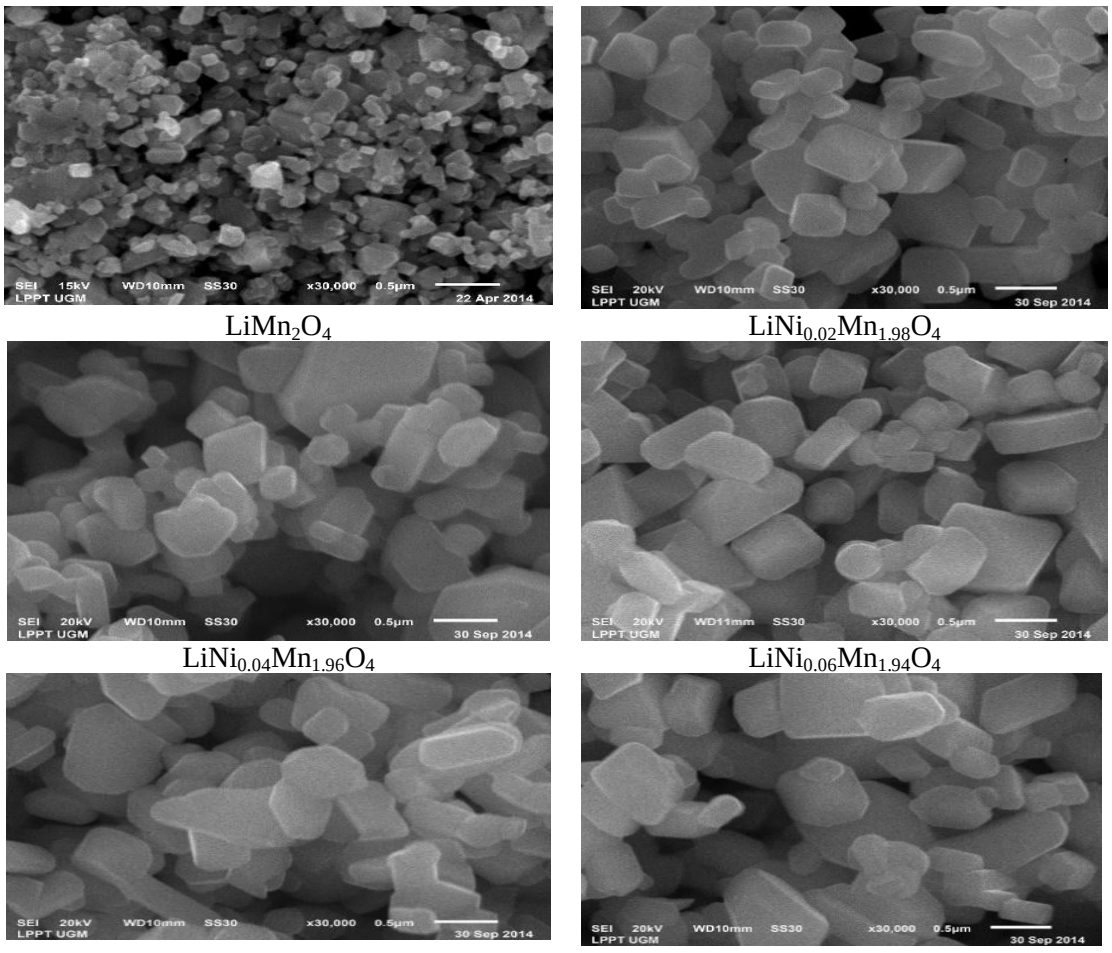

$LiMn_2O_4$ $LiNi_{0.02}Mn_{1.98}O_4$

$LiNi_{0.04}Mn_{1.96}O_4$ $LiNi_{0.06}Mn_{1.94}O_4$

$LiNi_{0.08}Mn_{1.92}O_4$ $LiNi_{0.10}Mn_{1.90}O_4$

Figure 5. SEM photographs of $LiNi_xMn_{2-x}O_4$

The SEM images of the synthesized powders are shown in Figure 5. The average particle size of the nickel-doped samples is smaller than that of undoped $LiMn_2O_4$. The doping of $LiNi_xMn_{2-x}O_4$ with Ni cause the tendency of nucleation process overcomes the tendency of crystal growth. The Ni-doped $LiMn_2O_4$ powders have irregular particle size. The particle sizes of $LiNi_xMn_{2-x}O_4$ are in the range of 150 to 500 nm. The increase in the nickel doping leads to increase in $LiMn_2O_4$ particle size. The morphology is almost similar.

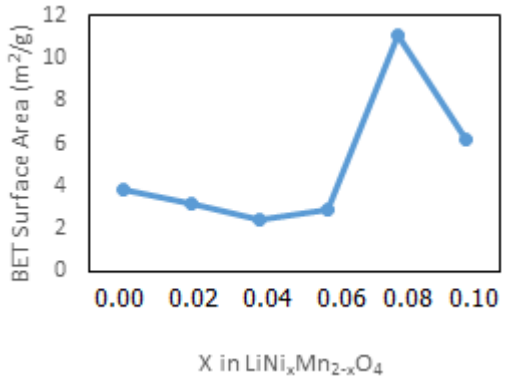

Figure 6. BET surface area of $LiNi_xMn_{2-x}O_4$

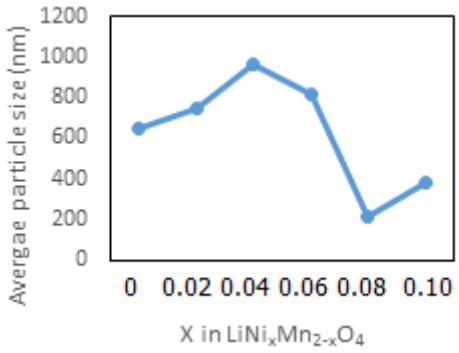

Figure 7. Variation of the average particle size with x in $LiNi_xMn_{2-x}O_4$

Figure 6 shows the BET surface area of $LiNi_xMn_{2-x}O_4$ at various mole ratios. The addition of Ni does not change the BET surface area. However, at a mole ratio of 0.08, there is a noticeable change in the BET surface area from 6 m^2/g to 11 m^2/g. Figure 7 shows the average particle size of the material. The particle size is in the range of 200-900 nm (Table 1). At low doping content, the particle size is relatively constant until it reaches x = 0.04. For x>0.04, the particle size decreases along with the increase of doping agent.The particle size is about 300 nm for x = 0.08. Good battery performance requires small particle size of cathodes [13]. In general, the particles have a rod shape. The particles are also agglomerated. The agglomerated particles might be beneficial for the production of lithium-ion batteries with high energy capacity [14]. A further test of the energy capacity of $LiNi_{0.08}Mn_{1.92}O_4$ is required. Calculation using Debye-Scherer equation gives crystallite size of $LiMn_{2-x}O_4$ in the range of 30-40 nm. The particle size obtained from the calculation (**) is around 200-900 nm.

Table 1. The crystallite size of the prepared materials as calculated by Debye-Scherer method, D, and the particle size as calculated from BET surface area data.

x	XRD	BET	
	D (nm)*	L (nm)**	$S_{BET}(m^2/g)$
0	39.42802	651.2078	3.6454
0.02	41.39063	746.8011	3.1756
0.04	43.1764	965.8867	2.4553
0.06	33.45325	817.3502	2.9015
0.08	36.38719	213.5754	11.104
0.1	36.21143	381.4117	6.2178

*$D= (K.\lambda)/B.\cos\Theta$

** $L= 6000/(\rho . S_{BET})$

4. Conclusion

$LiNi_xMn_{2-x}O_4$ has been synthesized by the low-temperature solid-state reaction. The $LiNi_xMn_{2-x}O_4$ powders have a cubic crystal structure with an *Fd3m* space group. The particle size of the prepared materials is not homogeneous. Doping with Ni leads to changes in size, crystallinity, and microstructure of the products. The average particle size of $LiNi_xMn_{2-x}O_4$ is about 150-500 nm. The crystallinity of the materials tends to increase with the increase in the Ni doping content. When Ni content in the compound increases, the lattice parameters decrease.

References

[1] Fergus J 2010 *J Power Sources* **195** 939-954
[2] Julien C M, Mauger A, Zaghib K and Groult H 2014 *Inorganics* **2** 132-154
[3] Hu M, Pang X and Zhou Z 2013 *J. Power Sources* **237** 229-242
[4] Peng C, Bai H, Xiang M, Su C, Liu G and Guo J 2014 *Int. J. Electrochem. Sci.* **9** 1791-1798
[5] Liu Q, Wang S, Tan H, Yang Z and Zeng J 2013 *Energies* **6** 1718-1730
[6] Guoqiang L 2010 $LiNi_{0.5}Mn_{1.5}O_4$ spinel and its derivatives as cathodes for Li-Ion batteries http://cdn.intechopen.com/pdfs-wm/29289.pdf
[7] Ding Y, Xie J, Cao G S, Zhu T J, Yu H M and Zhao X B 2011 *Adv. Func. Mat*. **21** 348-355
[8] Gu X, Li X, Xu L, Xu H, Yan J and Qian Y 2012 *Int. J. Electrochem. Sci* **7** 2504-2512
[9] Roisnel T and Ridriguez-Carvajal L 2001 in *WinPLOTR a graphic tool for powder diffraction*, CNRS-Lab. De Chimie du solide et inorganique moleculaire Universite de Rennes
[10] Brunauer S, Emmett P H and Teller E 1938 *J. of the American Chemical Society* **3** 309-319
[11] Purwaningsih D, Roto R, Narsito and Sutrisno H 2015 *Advanced Materials Re*search **1101** 134-137
[12] Li X 2009 *Journal of Alloys and Compounds* **479** 310-313
[13] Wang F X, Xiao S Y, Shi Y, Liu L L, Zhu Y S, Wu Y P, Wang J Z and Holze R 2013 Spinel $LiNi_xMn_{2-x}O_4$ as cathode material for aqueous rechargeable lithium batteries http://ro.uow.edu.au/aiimpapers/608
[14] Yi T, Xie Y, Ye M, Jiang L, Zhu R and Zhu Y 2011 *Ionics* **17** 383-389